

# Chapter 4

## Application of Detonation Waves to Rocket Engine Chamber

Jiro Kasahara, Yuichi Kato, Kazuaki Ishihara, Keisuke Goto, Ken Matsuoka, Akiko Matsuo, Ikkoh Funaki, Hideki Moriai, Daisuke Nakata, Kazuyuki Higashino, and Nobuhiro Tanatsugu

**Abstract** We present the results of experiments performed with a rotating detonation engine using continuous detonation in an annular combustor to create thrust. Detonation waves propagate in a supersonic and very small region, allowing shortening of the combustor. The combustor of RDE causes high-pressure loss when the propellant is injected, and cooling is necessary due to high heat flux. However, the combustion efficiency of detonation combustion in an annular combustor is the most important, but have not been fully elucidated. In addition, the influence of the injector shape and direct cooling of a rotating detonation combustor require clarification. This paper reports the measurement results of combustor stagnation pressure and thrust, the influence of injector shape on  $c^*$  efficiency, and the estimate of heat flux. The  $c^*$  efficiency was 88–100% when we used the convergent or convergent-divergent nozzle and the equivalence ratio was less than 1.0. The shape of the injector influenced wave propagation mode, but the mode did not change the  $c^*$  efficiency. We estimated time-spatial average heat flux from the terminal temperature, and the heat flux was  $8.1 \pm 1.8 \text{ MW/m}^2$  in no water injection condition. The rocket RDE sled test was successfully performed. The total mass of the rocket RDE system was 58.3 kg, total time averaged thrust was 201 N, the time averaged mass flow rate was 143 g/s, and the specific impulse was 144 s.

---

J. Kasahara (✉) • Y. Kato • K. Ishihara • K. Goto • K. Matsuoka  
Nagoya University, Nagoya, Aichi, Japan  
e-mail: [kasahara@nuae.nagoya-u.ac.jp](mailto:kasahara@nuae.nagoya-u.ac.jp)

A. Matsuo  
Keio University, Yokohama, Kanagawa, Japan

I. Funaki  
Japan Space Exploration Agency, Sagamihara, Kanagawa, Japan

H. Moriai  
Mitsubishi Heavy Industries Ltd., Komaki, Aichi, Japan

D. Nakata • K. Higashino • N. Tanatsugu  
Muroran Institute of Technology, Muroran, Hokkaido, Japan

## Nomenclature

$A_{inj}$	total injector area
$A_t$	throat area
$c^*$	characteristic velocity
$ER$	equivalence ratio
$F_t$	thrust
$g$	gravitational acceleration
$I_{sp}$	specific impulse
$M$	Mach number
$\dot{m}$	mass flow rate
$P$	pressure
$P_c$	combustor stagnation pressure
$R$	gas constant
$T$	temperature
$T_c$	adiabatic flame temperature

## Greek Symbols

$\gamma$	ratio of specific heat
$\eta_c$	$c^*$ efficiency

## Subscripts

i	ideal
m	measured

## 1 Introduction

A detonation wave is a combustion wave with pressure gain, which propagates at supersonic speed (2 ~ 3 km/s) into a combustible mixture. There are many fundamental studies of detonation wave engines (Kailasanath 2000, 2003; Wolański 2013; Lu and Braun 2014) and system level research studies (Kasahara et al. 2007; Hoke et al. 2010; Matsuoka et al. 2016; Frolov et al. 2013, 2015a, b; Dubrovskii et al. 2015). The detonation cycle has a higher thermal efficiency than a conventional gas turbine engine (Heiser and Pratt 2002; Wu et al. 2003; Talley and Coy 2002; Frolov et al. 2014; Nordeen 2013). Therefore, it is expected that a high-efficiency propulsion system can be realized using detonation waves.

A rotating detonation engine (RDE) uses continuous detonation in an annular combustor to create thrust. As detonation waves propagate at a supersonic speed in a very small region, the combustor can be shortened. The combustor of RDE causes high pressure loss when a propellant is injected, and cooling system is necessary due to high heat flux from the burned gas to the wall (Theuerkauf et al. 2015).

Some of the earliest RDE research was performed in the 1960s by the Russian scientist Voitsekhovskii (1960), Voitsekhovskii et al. 1967). In the 1990s, Bykovskii et al. (2006) studied air-breathing RDEs for a variety of gaseous and liquid fuels. There have also been many recent studies of RDE. Our research group performed visualization of rotating detonation waves (Nakayama et al. 2012; Nakagami et al. 2017a, b; Fujii et al. 2017; Gawahara et al. 2013), while Kato et al. (2016) and Ishihara et al. (2017) investigated thrust efficiency of the RDE. The CFD analysis (Hishida et al. 2009; Schwer and Kailasanath 2011, 2013), simplified steady state analysis (Fievisohn and Yu 2017), RDE experiments (Kindracki et al. 2011), thermodynamic modeling (Stechmann et al. 2017; Fotia et al. 2016), system level demonstration (Claffin 2012), rotating detonation turbine engine modeling (Paxson and Naples 2017), rotating detonation turbine engine demonstration (Naples et al. 2017) were performed.

The combustion efficiency and specific impulse of detonation combustion in an annular combustor are the most important physical parameters. Although the specific impulse meaning overall thrust performance of the RDE was investigated by many researchers, the combustion efficiency has not been investigated especially in the dependency on the mass flow rate of the propellant and injector geometries. In addition, the influence of the injector shape and direct cooling of a rotating detonation combustor require clarification. This paper reports the measurement results of combustor stagnation pressure and the influence of injector shape on  $c^*$  efficiency. We then performed cooling by injecting water directly into the combustor and measured the heat flux on the surface of the outer combustor.

## 2 Experimental Apparatus

The RDE used in this study is shown in Fig. 4.1. The RDE was made of copper (C1100) in purpose of thermal diffusion. The inner diameter of the annular combustor was 60.5 mm, the width 3.2 mm, and the axial length 48 mm. The RDE had a 30° conical plug, and a detachable convergent nozzle and divergent nozzle. The contraction ratio was 1.25, and the expansion ratio was 2.0 (there is no optimization for this ratios). We used gaseous ethylene and gaseous oxygen as the propellants. Oxidizer ( $O_2$ ) mass flow rate is much larger than fuel ( $C_2H_4$ ), then generally oxidizer plenum pressure is higher than fuel. Since oxidizer plenum characteristic length should be smaller, in this experiment the oxidizer ( $O_2$ ) is injected from the center plenum whereas the fuel ( $C_2H_4$ ) is injected at a larger outer radius.

**Fig. 4.1** Schematic of annular detonation combustor (sectional view)

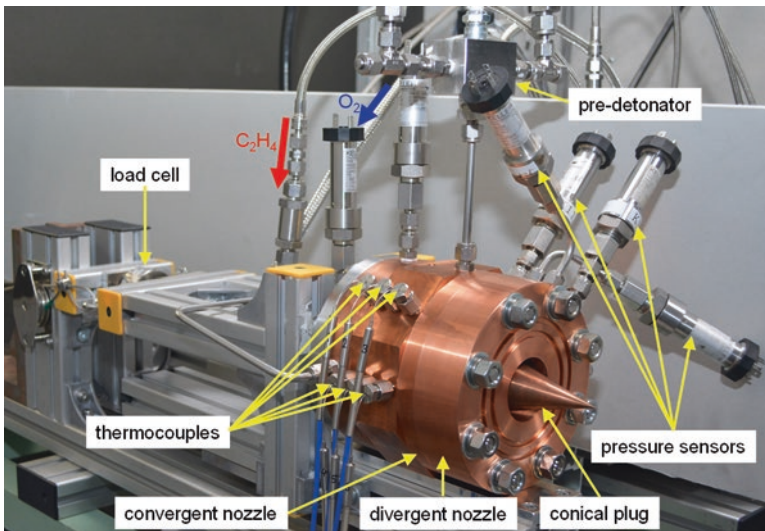
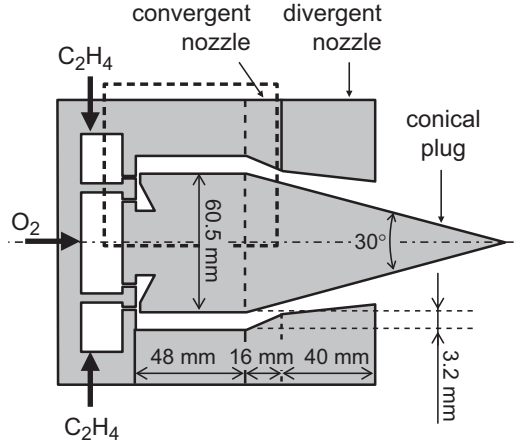


**Fig. 4.2** Photograph of experimental apparatus of the RDE

Figure 4.2 shows photograph of the RDE experimental apparatus. We used pre-detonator tube on the side wall of the annular combustor. We also set the load cell on the bottom of the RDE system for measuring the thrust as shown in Fig. 4.2.

Figure 4.3 is an enlarged view of the RDE. We used two types of injectors (type 1, type 2). Type 1 had 72 fuel injection holes of 0.66-mm diameter and a 1-mm wide oxidizer injection slot. In type 2, the 72 fuel injection holes were 0.50 mm in diameter, and the oxidizer injection slot was 0.3-mm wide. Pressure sensors were inserted in the fuel and oxidizer plenums. Each type had pressure ports (2.0 mm diameter),  $P_1$ ,  $P_2$ , and we measured local static pressure. In type 2, there were pressure ports (0.5 mm diameter),  $P_{0,1}$ ,  $P_{0,2}$ , located at bottom of the combustor to obtain combustor stagnation pressure.

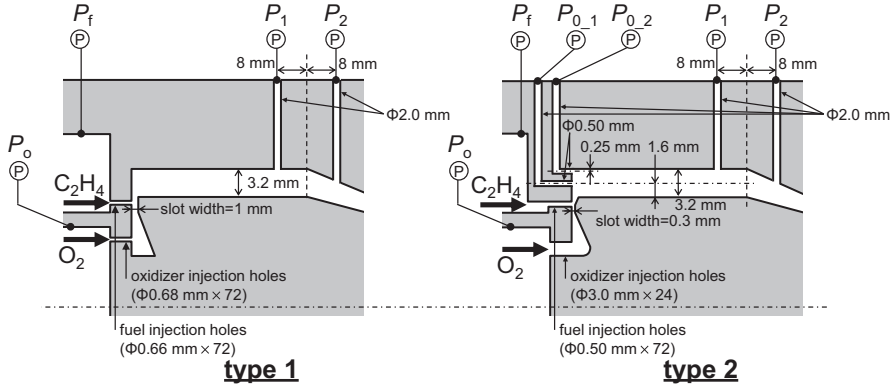


Fig. 4.3 Enlarged view of the RDE combustor: *left*, type 1; *right*, type 2

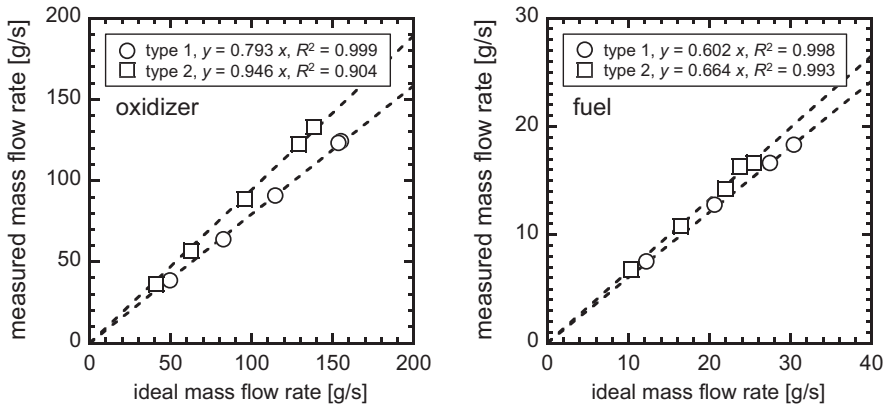


Fig. 4.4 Result of mass flow rate calibration: *left*, oxidizer; *right*, fuel

### 3 Experimental Results and Discussion for Combustion Chamber

We performed mass flow calibration by blowing down cold gas, fuel and oxidizer separately. The mass flow rate was adjusted by the initial tank pressure or the orifice diameter located in upper flow. Figure. 4.4 shows the results of mass flow rate calibration. Ideal mass flow rate,  $\dot{m}_i$ , was calculated from plenum pressure in choked condition at the injectors as follows:

$$\dot{m}_i = \frac{PA_{inj}}{\sqrt{RT}} \sqrt{\gamma \left( \frac{2}{\gamma + 1} \right)^{\frac{\gamma + 1}{\gamma - 1}}} \quad (4.1)$$

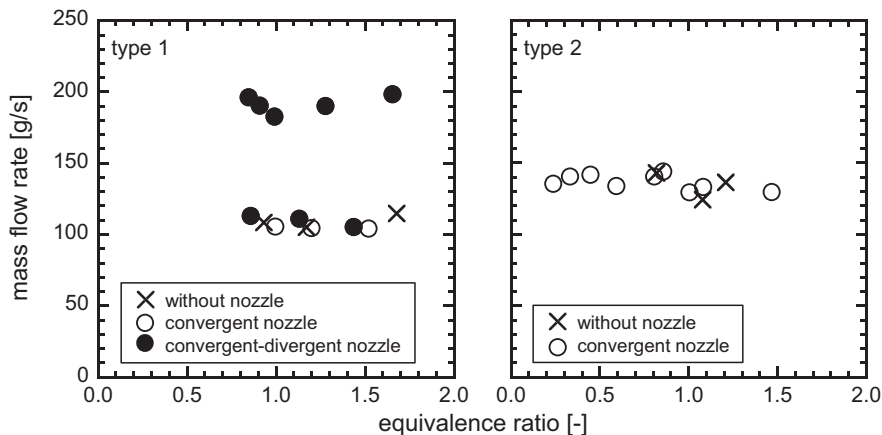


Fig. 4.5 Experimental conditions: *left*, type 1; *right*, type 2

Measured mass flow rate was determined from operation duration and tank mass decrease. The tank mass decrease was determined by an electronic balance or the internal tank pressure decrease. In the combustion test, we determined ideal mass flow rate from plenum pressure, and actual mass flow was obtained using the relationship in Fig. 4.4.

Figure 4.5 shows the experimental conditions. We changed mass flow rate ( $108 \pm 4$  g/s,  $136 \pm 6$  g/s,  $191 \pm 6$  g/s), equivalence ratio (0.24–1.68), injector (type 1, type 2), and nozzle (without, convergent, convergent-divergent).

Figure 4.6 presents the visualization result by high-speed camera (SA5, 150,000 fps). Intermittent bright waves were observed in type 1, and thrust was obtained and combustion was kept in the combustor. On the other hand 2 or 3 waves were observed in type 2. Wave propagation speed was 2040 m/s (84% of C-J speed) or 1750 m/s (72% of C-J speed). The lower speed than CJ wave maybe due to insufficient mixing and large wave curvature effect. Thus, injector shape influenced wave propagation mode. There are transient phenomena from two waves to three waves in the type 2 injector case shown in the right of Fig. 4.6. The new wave generates in the two-wave mode. It is due to mass flow rate disturbances at the starting process of the RDE operation. For simplicity, we show only the data points which can be clearly correspond to two or three wave mode.

Figure 4.7 shows the pressure and thrust history in the combustion test using the convergent nozzle. In the type 1 configuration, the injector is hole type only. Otherwise, in the type 2 configuration, the injector of the oxygen is slit type. The slit width is decreasing during the operation due to thermal deformation (expansion) of the inner wall of the RDE. Therefore the pressure in the oxygen plenum increases for the type 2 configuration but remains fairly constant for the type 1 configuration. Thrust was measured by a load cell and average thrust during the operation is drawn as dashed lines. The load cell used in this experiment was AIKOH DUD-200 K, and its maximum frequency response is 500 Hz. The average thrust was 142 N in type

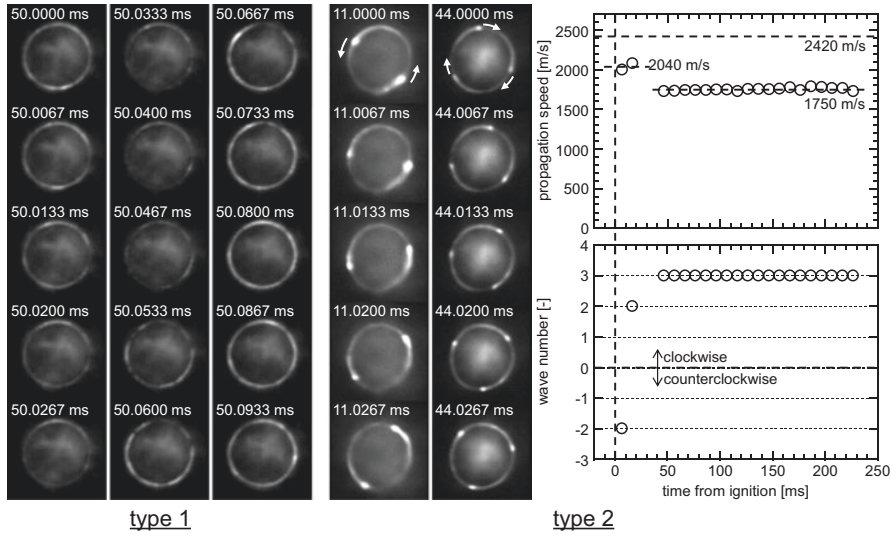


Fig. 4.6 Visualization by high-speed camera: *left*, type 1 ( $\dot{m}=105$  g/s,  $ER = 1.17$ , without nozzle); *right*, type 2 ( $\dot{m}=125$  g/s,  $ER = 1.08$ , without nozzle)

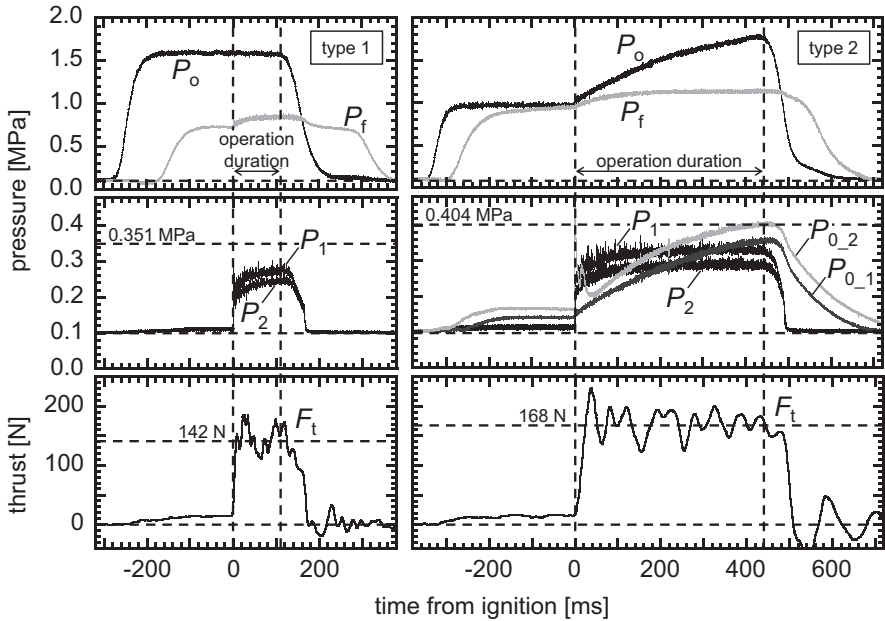


Fig. 4.7 Pressure and thrust history: *left*, type 1 ( $\dot{m}=105$  g/s,  $ER = 1.00$ , convergent nozzle); *right*, type 2 ( $\dot{m}=134$  g/s,  $ER = 0.60$ , convergent nozzle)

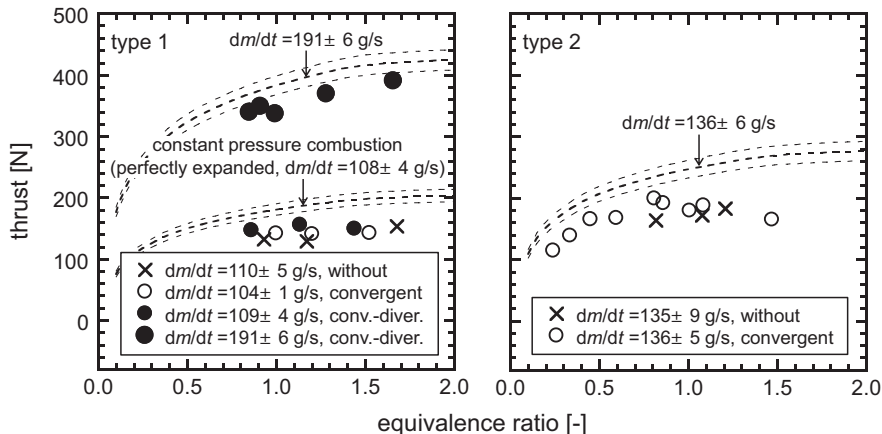


Fig. 4.8 Thrust vs. equivalence ratio: *left*, type 1; *right*, type 2

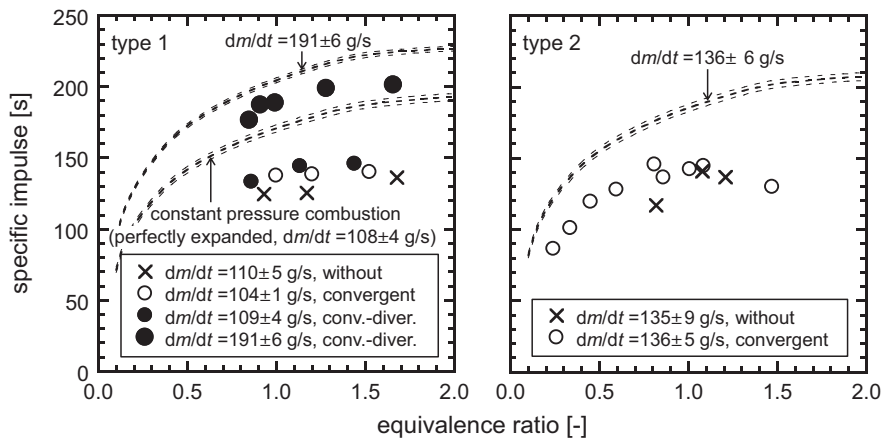


Fig. 4.9 Specific impulse vs. equivalence ratio: *left*, type 1; *right*, type 2

1, and 168 N in type 2. Mass flow rate was determined by using plenum pressure before the ignition.

Figure 4.8 shows the thrust vs. equivalence ratio. Figure 4.9 shows the specific impulse vs. equivalence ratio. Specific impulse,  $I_{sp}$ , was defined as follows:

$$I_{sp} \equiv \frac{F_t}{\dot{m}g} \tag{4.2}$$

Dashed lines indicate the ideal value of the constant pressure combustion rocket engine. In calculating the value, the throat area was equal to the experimental apparatus, and the burned gas was perfectly expanded and frozen in the nozzle. The



thrust was 115–391 N, the specific impulse was 87–201 s. By using convergent nozzle thrust increased approximately 10% compared with the combustor without nozzle. Thrust efficiency might increase because of higher combustor pressure. In convergent-divergent nozzle condition, thrust was 10–17% higher than the combustor without nozzle. In case of low mass flow rate ( $109 \pm 4$  g/s), overexpansion occurred. When the mass flow rate was  $191 \pm 6$  g/s, we had already achieved 88–94% efficiency as compared to the ideal value so that burned gas was almost perfectly expanded.

In the RDE combustor, the flow is essentially unsteady state and three dimensional. However, in this experiment, experimental input (plenum pressure and mass flow rate) and experimental output (thrust of RDE) were kept almost steady state relative to the RDE unsteady phenomena, as shown in Figs. 4.7 and 4.8. Therefore, for simplicity, the following one or quasi-one steady-state flow in RDE combustor are assumed.

At first, we calculated the ideal combustor stagnation pressure. Gas constant, adiabatic flame temperature, and ratio of specific heat were determined by NASA-CEA. Ideal combustor stagnation pressure,  $P_{c,i}$ , was obtained as follows:

$$P_{c,i} = \frac{\dot{m} \sqrt{RT_c}}{A_t \sqrt{\gamma \left( \frac{2}{\gamma+1} \right)^{\frac{\gamma+1}{\gamma-1}}}} \quad (4.3)$$

Next we obtained combustor stagnation pressure in the experiment. The Mach number at the  $P_1$  port was determined as follows:

$$\frac{A}{A_t} = \frac{1}{M} \left\{ \frac{(\gamma-1)M^2 + 2}{\gamma+1} \right\}^{\frac{\gamma+1}{2(\gamma-1)}} \quad (4.4)$$

The ratio of specific heat was determined by NASA-CEA and assumed to be constant. Measured combustor stagnation pressure,  $P_{c,m}$ , was obtained as follows:

$$P_{c,m} = P_1 \left( 1 + \frac{\gamma-1}{2} M^2 \right)^{\frac{\gamma}{\gamma-1}} \quad (4.5)$$

The characteristic velocity,  $c^*$ , and characteristic-velocity efficiency,  $\eta_{c^*}$ , were then defined as follows:

$$c^* \equiv \frac{P_c A_t}{\dot{m}} \quad (4.6)$$

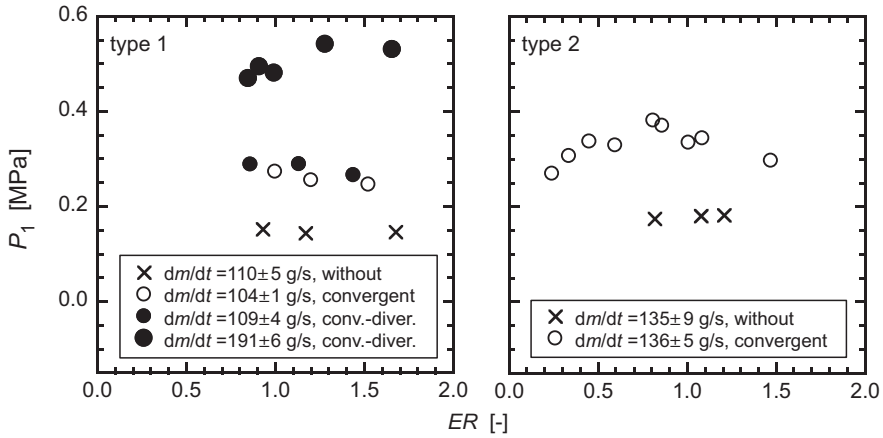


Fig. 4.10 Combustor pressure,  $P_1$  vs. equivalence ratio: left, type 1; right, type 2

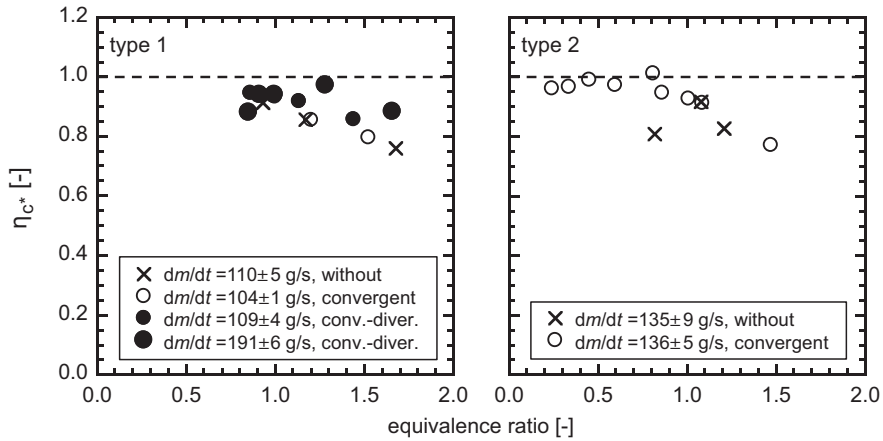


Fig. 4.11  $c^*$  efficiency calculated from  $P_1$  vs. equivalence ratio: left, type 1; right, type 2

$$\eta_{c^*} \equiv \frac{c_m^*}{c_i^*} = \frac{P_{c-m}}{P_{c-i}} \tag{4.7}$$

Figure 4.10 shows the combustor pressure,  $P_1$  vs. equivalence ratio, and Fig. 4.11 shows the  $c^*$  efficiency calculated from  $P_1$  vs. the equivalence ratio. Pressure increase was obtained using either the convergent or convergent-divergent nozzle. We compare type 1 and 2 in Fig. 11; there was little difference in  $c^*$  efficiency. The injector shape influenced wave propagation mode, but the mode could not change the  $c^*$  efficiency. When we used the convergent or convergent-divergent nozzle and the equivalence ratio was less than 1.0,  $c^*$  efficiency was 88–101%. If both combustor pressure and oxidizer mass flow rate were high, there was a tendency for the

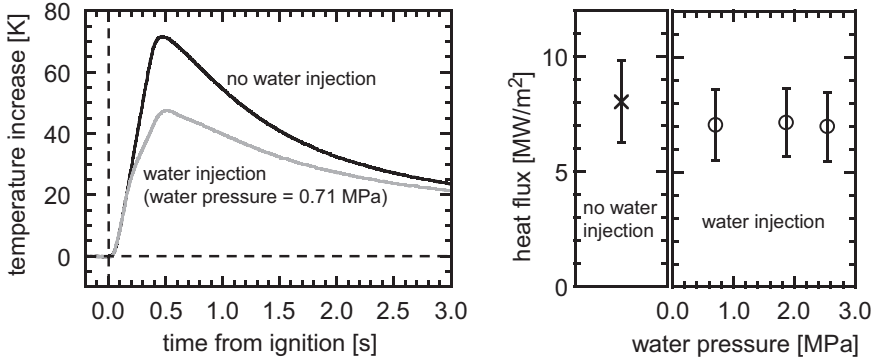


Fig. 4.12 Temperature increase history and heat flux vs. water pressure

efficiency to be high. Then as combustor pressure,  $P_{0,2}$ , asymptotically approached the ideal line in Fig. 4.7, we concluded that the combustor stagnation pressure could be directly measured at the bottom corner of the combustor.

Cooling tests by directly injecting water into the combustor through a hole of diameter of 0.5 mm was carried out for development of cooling system of a RDE. Figure 4.12 shows temperature increase history and heat flux versus water pressure. The temperature was measured by a sheath type thermocouple (0.5 mm diameter) which was inserted into a hole in the combustor outer. The distance between the bottom of the hole and the combustor outer surface was 2 mm. Combustion was kept during water injection, and local temperature increase rate was decreased. And we estimated time-spatial average heat flux into the ambient from the terminal temperature, and the heat flux was  $8.1 \pm 1.8$  MW/m<sup>2</sup> with no water injection. There is not much of a difference between no water injection and water injection. The water injector hole is only one, and then the distribution of the water is not homogeneous. The water may be diffused to wider region by the unsteady RDE combustor flow than a conventional relatively steady combustor flow. These effect (small mass flow rate water spreads wider region) causes small heat flux difference between the two cases.

## 4 Experimental Results and Discussion for RDE System Sled Test

For demonstrating rocket RDE system, the sled test of this system was performed at Muroran Institute of Technology in Japan. Figures 4.13 and 4.14 show the pictures of the rocket RDE system for a sled test. As shown in Fig. 4.13, all the devices of the system were located on the flat aluminum alloy plate (1000 mm length and 30 mm width).

As shown in Fig. 4.14, the rocket RDE system was sledged on 5-inch rails of total length of 100 m. The rocket RDE system was supported by four wheels.

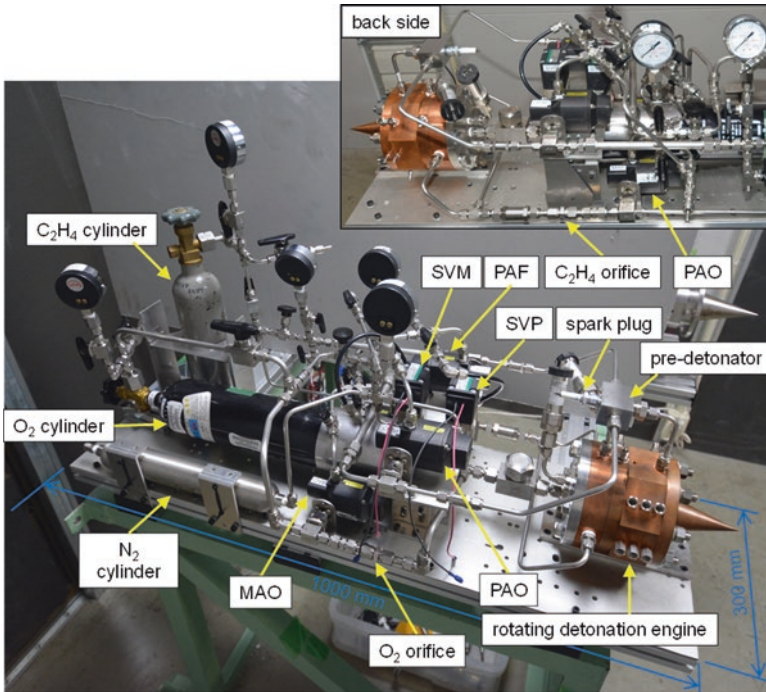


Fig. 4.13 Piping system picture of the rocket RDE system

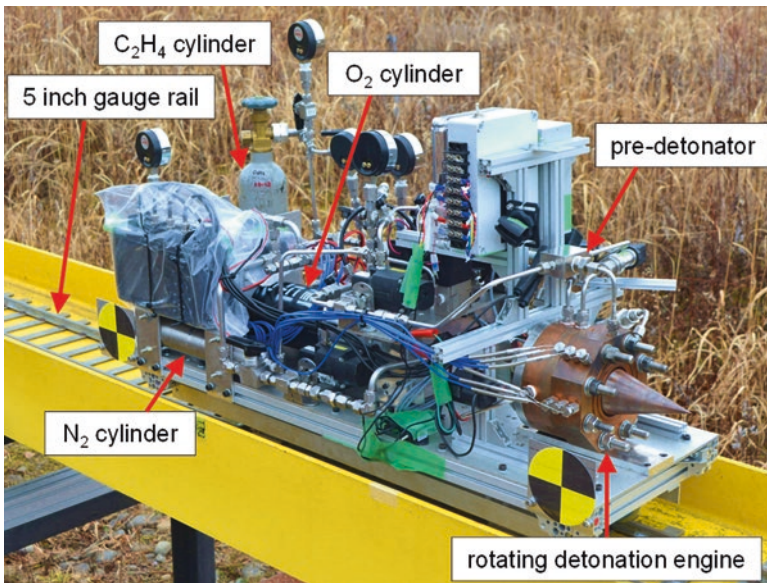
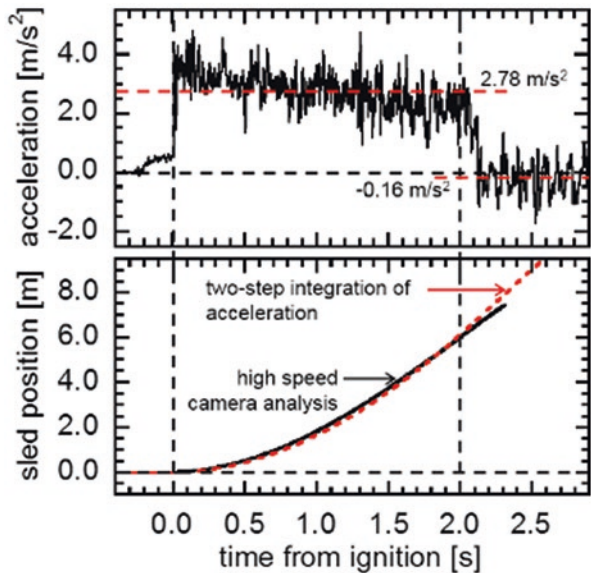


Fig. 4.14 Picture of the rocket RDE system for a sled test



**Fig. 4.15** The RDE sled test was successfully performed

**Fig. 4.16** The acceleration and position of the system. The total time averaged acceleration was  $2.94 = 2.78 + 0.16$  ( $\text{m/s}^2$ )



The rocket RDE sled test was successfully performed as shown in Fig. 4.15. The operation time was two seconds and the total sled distance was 70.22 m. As shown in Fig. 4.16, the time averaged acceleration was  $2.78 \text{ m/s}^2$ . But, time averaged deceleration by friction was estimated as  $-0.16 \text{ m/s}^2$  using observation of the deceleration

after closing the engine thrust. Thus, total thrust can be estimated  $2.93 \text{ m/s}^2$ . As the total mass of the system was 58.3 kg, total time averaged thrust was 201 N. The time averaged mass flow rate was 143 g/s. The specific impulse was 144 s.

## 5 Conclusions

We performed combustion tests of RDE with convergent-divergent nozzle using gaseous ethylene and oxygen as the propellant, measured the combustor pressure, and determined the  $c^*$  efficiency. The efficiency was 88–100% when we used the convergent or convergent-divergent nozzle and the equivalence ratio was less than 1.0. The shape of the injector influenced wave propagation mode, but the mode did not change the  $c^*$  efficiency. We estimated time-spatial average heat flux from the terminal temperature, and the heat flux was  $8.1 \pm 1.8 \text{ MW/m}^2$  in no water injection. The rocket RDE sled test was successfully performed. The total mass of the rocket RDE system was 58.3 kg, total time averaged thrust was 201 N, the time averaged mass flow rate was 143 g/s, and the specific impulse was 144 s.

**Acknowledgements** The present RDE development was subsidized by a “Study on Innovative Detonation Propulsion Mechanism,” Research-and-Development Grant Program (Engineering) from the Institute of Space and Astronautical Science, the Japan Aerospace Exploration Agency. The fundamental device development was subsidized by a Grant-in-Aid for Scientific Research (A), No. 24246137.

## References

- Bykovskii, F. A., Sergey, Z. A., & Vedernikov, E. F. (2006). Continuous spin detonations. *Journal of Propulsion and Power*, 22(6), 1204–1216.
- Claffin, S. (2012). *Recent progress in continuous detonation engine development at Pratt & Whitney Rocketdyne*. Paper presented at International Workshop on Detonation for Propulsion 2012, Tsukuba, 3–5 September 2012.
- Dubrovskii, A. V., Ivanov, V. S., & Frolov, S. M. (2015). Three-dimensional numerical simulation of the operation process in a continuous detonation combustor with separate feeding of hydrogen and air. *Russian Journal of Physical Chemistry B*, 9(1), 104–119.
- Fievisohn, R. T., & Yu, K. H. (2017). Steady-state analysis of rotating detonation engine flowfields with the method of characteristics. *Journal of Propulsion and Power*, 33(1), 89–99.
- Fotia, M. L., Kaemming, T. A., Hoke, J. L., and Schauer, F. (2016). *Thermodynamics modelling and the operation of rotating detonation engines at elevated inlet temperatures*. Paper presented at 2016 International Workshop on Detonation for Propulsion, Temasek Laboratories, National University of Singapore, 12–15 July 2016.
- Frolov, S. M., Dubrovskii, A. V., & Ivanov, V. S. (2013). Three-dimensional numerical simulation of the operation of a rotating-detonation chamber with separate supply of fuel and oxidizer. *Russian Journal of Physical Chemistry B*, 7(1), 35–43.
- Frolov, S. M., Aksenov, V. S., Gusev, P. A., Ivanov, V. S., Medvedev, S. N., & Shamshin, I. O. (2014). Experimental proof of the energy efficiency of the Zel'dovich thermodynamic cycle. *Doklady Physical Chemistry*, 459(2), 207–211.

- Frolov, S. M., Aksenov, V. S., & Ivanov, V. S. (2015a). Experimental proof of Zel'dovich cycle efficiency gain over cycle with constant pressure combustion for hydrogen–oxygen fuel mixture. *International Journal of Hydrogen Energy*, *40*(21), 6970–6975.
- Frolov, S. M., Aksenov, V. S., Ivanov, V. S., & Shamshin, I. O. (2015b). Large-scale hydrogen–near continuous detonation combustor. *International Journal of Hydrogen Energy*, *40*(3), 1616–1623.
- Fujii, J., Kumazawa, Y., Matsuo, A., Nakagami, S., & Kasahara, J. (2017). Numerical investigation on velocity deficit of detonation wave in RDE chamber. *Proceedings of the Combustion Institute*, *36*(2), 2665–2672.
- Gawahara, K., Nakayama, H., Kasahara, J., Tomioka, S., & Hiraiwa, T. (2013). *Detonation engine development for reaction control systems of a spacecraft*. Paper presented at 49th AIAA/ASME/SAE/ASEE Joint Propulsion Conference & Exhibit and 11th International Energy Conversion Engineering Conference, AIAA-2013–3721, San Jose Convention Center, San Jose, July 15–17, 2013.
- Heiser, W. H., & Pratt, D. T. (2002). Thermodynamic cycle analysis of pulse detonation engines. *Journal of Propulsion and Power*, *18*(1), 68–76.
- Hishida, M., Fujiwara, T., & Wolański, P. (2009). Fundamentals of rotating detonations. *Shock Waves*, *19*(1), 1–10.
- Hoke, J. L., Bradley, R. P., Brown, A. C., Litke, P. J., Stutrud, J. S., and Schauer, F. R. (2010). *Development of a pulse detonation engine for flight*. Paper presented at Symposium on Shock Waves in Japan (pp. 239–246).
- Ishihara, K., Nishimura, J., Goto, K., Nakagami, S., Matsuoka, K., Kasahara, J., Matsuo, A., and Funaki, I. (2017). *Study on a long-time operation towards rotating detonation rocket engine flight demonstration*. Paper presented at SciTech 2017, 55<sup>th</sup> AIAA Aerospace Science Meeting, AIAA 2017–1062, Grapevine, Texas, USA, January 8–12, 2017.
- Kailasanath, K. (2000). Review of propulsion applications of detonation waves. *AIAA Journal*, *38*(9), 1698–1708.
- Kailasanath, K. (2003). Recent developments in the research on pulse detonation engines. *AIAA Journal*, *41*(2), 145–159.
- Kasahara, J., Hasegawa, A., Nemoto, T., Yamaguchi, H., Yajima, T., & Kojima, T. (2007). Performance validation of a single-tube pulse detonation rocket system. *Journal of Propulsion and Power*, *25*(1), 173–180.
- Kato, Y., Ishihara, K., Matsuoka, K., Kasahara, J., Matsuo, A., and Funaki, I. (2016). *Study of combustion chamber characteristic length in rotating detonation engine with convergent-divergent nozzle*. Paper presented at 54th AIAA Aerospace Sciences Meeting, AIAA 2016–1406, San Diego, January 4–8, 2016.
- Kindracki, J., Wolański, P., & Gut, Z. (2011). Experimental research on the rotating detonation in gaseous fuels–oxygen mixtures. *Shock Waves*, *21*(2), 75–84.
- Lu, F. K., & Braun, E. M. (2014). Rotating detonation wave propulsion: experimental challenges, modeling, and engine concepts. *Journal of Propulsion and Power*, *30*(5), 1125–1142.
- Matsuoka, K., Morozumi, T., Takagi, S., Kasahara, J., Matsuo, A., & Funaki, I. (2016). Flight validation of a rotary-valved four-cylinder pulse detonation rocket. *Journal of Propulsion and Power*, *32*(2), 383–391.
- Nakagami, S., Matsuoka, K., Kasahara, J., Kumazawa, Y., Fujii, J., Matsuo, A., & Funaki, I. (2017a). Experimental visualization of the structure of rotating detonation waves in a disk-shaped combustor. *Journal of Propulsion and Power*, *33*(1), 80–88.
- Nakagami, S., Matsuoka, K., Kasahara, J., Matsuo, A., & Funaki, I. (2017b). Experimental study of the structure of forward-tilting rotating detonation waves and highly maintained combustion chamber pressure in a disk-shaped combustor. *Proceedings of the Combustion Institute*, *36*(2), 2673–2680.
- Nakayama, H., Moriya, T., Kasahara, J., Matsuo, A., Sasamoto, Y., & Funaki, I. (2012). Stable detonation wave propagation in rectangular-cross-section curved channels. *Combustion and Flame*, *159*(2), 859–869.

- Nordeen, C. A. (2013). *Thermodynamics of a rotating detonation engine*, doctoral dissertations, University of Connecticut, 2013.
- Naples, A., Hoke, J., Battelle, R., Wagner, M., and Schauer, F. (2017). *Rotating detonation engine implementation into an open-loop T63 gas turbine engine*. Paper presented at 55th AIAA Aerospace Sciences Meeting, AIAA 2017-1747, Grapevine, 9-13 January, 2017.
- Paxson, D. E. and Naples, A. (2017). *Numerical and analytical assessment of a coupled rotating detonation engine and turbine experiment*. Paper presented at 55th AIAA Aerospace Sciences Meeting, AIAA 2017-1746, Grapevine, 9-13 January, 2017.
- Schwer, D., & Kailasanath, K. (2011). Numerical investigation of the physics of rotating-detonation-engines. *Proceedings of the Combustion Institute*, 33(2), 2195-2202.
- Schwer, D., & Kailasanath, K. (2013). Fluid dynamics of rotating detonation engines with hydrogen and hydrocarbon fuels. *Proceedings of the Combustion Institute*, 34(2), 1991-1998.
- Stechmann, D., Heister, S. D., and Sardeshmukh, S. (2017). *High-pressure rotating detonation engine testing and flameholding analysis with hydrogen and natural gas*. Paper presented at 55th AIAA Aerospace Sciences Meeting, AIAA 2017-1931, Grapevine, 9-13 January, 2017.
- Theuerkauf, S. W., Schauer, F. R., Anthony, R., and Hoke, J. L. (2015). *Experimental characterization of high-frequency heat flux in a rotating detonation engine*. Paper presented at 53rd AIAA Aerospace Science Meeting, AIAA 2015-1603, Kissimmee, 5-9 January, 2015.
- Talley, D. G., & Coy, E. B. (2002). Constant volume limit of pulsed propulsion for a constant  $\gamma$  ideal gas. *Journal of Propulsion and Power*, 18(2), 400-406.
- Voitsekhovskii, B. V. (1960). Stationary spin detonation. Soviet. *Journal of Applied Mechanics and Technical Physics*, 3, 157-164.
- Voitsekhovskii, B. V., Mitrofanov, V. V., & Topchian, M. E. (1967). Investigation of the structure of detonation waves in gases. *Symposium (International) on Combustion*, 12(1), 829-837.
- Wolan'ski, P. (2013). Detonative propulsion. *Proceedings of the Combustion Institute*, 34(1), 125-158.
- Wu, Y., Ma, F., & Yang, V. (2003). System performance and thermodynamic cycle analysis of air-breathing pulse detonation engines. *Journal of Propulsion and Power*, 19(4), 556-567.